

1 **Effect of elevated $p\text{CO}_2$ on trace gas production during an**
2 **ocean acidification mesocosm experiment**

3 Sheng-Hui Zhang^{1,3§}, JuanYu^{1,2§}, Qiong-Yao Ding¹, Hong-Hai Zhang^{1,2}, Gui-Peng Yang^{1,2*},
4 Kun-Shan Gao⁴, Da-Wei Pan³

5 ¹ Key Laboratory of Marine Chemistry Theory and Technology, Ministry of Education, Ocean
6 University of China, Qingdao 266100, China

7 ² Laboratory for Marine Ecology and Environmental Science, Qingdao National Laboratory for
8 Marine Science and Technology, Qingdao 266237, China

9 ³ Key Laboratory of Coastal Environmental Processes and Ecological Remediation, Yantai
10 Institute of Coastal Zone Research (YIC), Chinese Academy of Sciences(CAS); Shandong
11 Provincial Key Laboratory of Coastal Environmental Processes, YICCAS, Yantai Shandong
12 264003, P. R. China

13 ⁴ State Key Laboratory of Marine Environmental Science, Xiamen University, Xiamen, 361102,
14 China

15 * Corresponding author:

16 Prof. Gui-Peng Yang
17 Key Laboratory of Marine Chemistry Theory and Technology
18 Ocean University of China
19 Qingdao 266100

20 China

21 E-mail: gpyang@mail.ouc.edu.cn

22 Tel: +86-532-66782657

23 Fax: +86-532-66782657

24 Author contributions

25 §Sheng-Hui Zhang and JuanYu contributed equally

26

27

28

29

30

31 **Abstract**

32 A mesocosm experiment was conducted in Wuyuan Bay (Xiamen), China to investigate the effects of elevated
33 $p\text{CO}_2$ on phytoplankton species and production of dimethylsulfide (DMS), dimethylsulfoniopropionate (DMSP)
34 and DMSP-consuming bacteria (DCB) as well as four halocarbon compounds (CHBrCl_2 , CH_3Br , CH_2Br_2 , and
35 CH_3I). Over a period of 5 weeks, *Phaeodactylum tricorunatum* outcompeted *Thalassiosira weissflogii* and
36 *Emiliana huxleyi*, comprising more than 99% of the final biomass. During the logarithmic growth phase (phase I),
37 DMS concentrations in high $p\text{CO}_2$ mesocosms (HC, 1000 μatm) were 28% lower than those in low $p\text{CO}_2$
38 mesocosms (LC, 400 μatm). Elevated $p\text{CO}_2$ led to a delay in DCB concentrations attached to *Thalassiosira*
39 *weissflogii* and *Phaeodactylum tricorunatum* and finally resulted in the delay of DMS concentration in the HC
40 treatment. Unlike DMS, the elevated $p\text{CO}_2$ did not affect DMSP production ability of *Thalassiosira weissflogii* or
41 *Phaeodactylum tricorunatum* throughout the 5 weeks culture. A positive relationship was detected between CH_3I
42 and *Thalassiosira weissflogii* and *Phaeodactylum tricorunatum* during the experiment, and there was a 40%
43 reduction in mean CH_3I concentrations in the HC mesocosms. CHBrCl_2 , CH_3Br , and CH_2Br_2 concentrations did
44 not increase with elevated chlorophyll *a* (Chl *a*) concentrations compared with DMS(P) and CH_3I , and there were
45 no major peaks both in the HC or LC mesocosms. In addition, no effect of elevated $p\text{CO}_2$ was identified for any of
46 the three bromocarbons.

47 **Keywords:** ocean acidification, dimethylsulfide (DMS), dimethylsulfoniopropionate (DMSP), halocarbons,
48 phytoplankton, bacteria

49

50

51

52 **1. Introduction**

53 Anthropogenic emissions have increased the fugacity of atmospheric carbon dioxide ($p\text{CO}_2$) from
54 the pre-industrial value of 280 μatm to the present-day value of over 400 μatm , and these values
55 will further increase to 800–1000 μatm by the end of this century (Gattuso et al., 2015). The
56 dissolution of this excess CO_2 into the surface of the ocean directly affects the carbonate system
57 and has lowered the pH by 0.1 units, from 8.21 to 8.10 over the last 250 years. Further decreases
58 of 0.3–0.4 pH units are predicted by the end of this century (Doney et al., 2009; Orr et al., 2005;
59 Gattuso et al., 2015), which is commonly referred to as ocean acidification (OA). The
60 physiological and ecological aspects of the phytoplankton response to this changing environment
61 can potentially alter marine phytoplankton community composition, community biomass, and
62 feedback to biogeochemical cycles (Boyd and Doney, 2002). These changes simultaneously have
63 an impact on some volatile organic compounds produced by marine phytoplankton (Liss et al.,
64 2014; Liu et al., 2017), including the climatically important trace gas dimethylsulfide (DMS) and
65 a number of volatile halocarbon compounds.

66 DMS is the most important volatile sulfur compound produced from
67 dimethylsulfoniopropionate (DMSP), which is ubiquitous in marine environments, mainly
68 synthesized by marine microalgae (Stefels et al., 2007), a few angiosperms, some corals (Raina et
69 al., 2016), and several heterotrophic bacteria (Curson et al., 2017) through complex biological
70 interactions in marine ecosystems. Although it remains controversial, DMS and its by-products,
71 such as methanesulfonic acid and non-sea-salt sulfate, are suspected to have a prominent part in
72 climate feedback (Charlson et al., 1987; Quinn and Bates, 2011). The conversion of DMSP to
73 DMS is facilitated by several enzymes, including DMSP-lyase and acyl CoA transferase

74 (Kirkwood et al., 2010; Todd et al., 2007); these enzymes are mainly found in phytoplankton,
75 macroalgae, *Symbiodinium*, bacteria and fungi (de Souza and Yoch, 1995; Stefels and Dijkhuizen,
76 1996; Steinke and Kirst, 1996; Bacic and Yoch, 1998; Yost and Mitchelmore, 2009). Several
77 studies have shown a negative impact of decreasing pH on DMS-production capability (Hopkins
78 et al., 2010; Avgoustidi et al., 2012; Archer et al., 2013; Webb et al., 2016), while others have
79 found either no effect or a positive effect (Vogt et al., 2008; Hopkins and Archer, 2014). Several
80 assumptions have been presented to explain these contrasting results and attributed the
81 pH-induced variation in DMS-production capability to altered physiology of the algae cells or of
82 bacterial DMSP degradation (Vogt et al., 2008; Hopkins et al., 2010, Avgoustidi et al., 2012;
83 Archer et al., 2013; Hopkins and Archer, 2014; Webb et al., 2015).

84 Halocarbons also play a significant role in the global climate because they are linked to
85 tropospheric and stratospheric ozone depletion and a synergistic effect of chlorine and bromine
86 species has been reported that they may account for approximately 20% of the polar stratospheric
87 ozone depletion (Roy et al., 2011). In addition, iodocarbons can release atomic iodine (I) quickly
88 through photolysis in the atmospheric boundary layer and I atoms are very efficient in the catalytic
89 removal of O₃, which governs the lifetime of many climate relevant gases including methane and
90 DMS (Jenkins et al., 1991). Compared with DMS, limited attention was received about the effect
91 of OA on halocarbon concentrations. Hopkins et al. (2010) and Webb et al. (2015) measured lower
92 concentrations of several iodocarbons, while bromocarbons were unaffected by elevated pCO₂
93 through two acidification experiments. In addition, an additional mesocosm study did not elicit
94 significant differences from any halocarbon compounds at up to 1,400 μatm pCO₂ (Hopkins et al.,
95 2013).

96 DMS and halocarbons play a significant role in the global climate and perhaps act a greater
97 extent in the future. Meanwhile, the combined picture arising from existing studies is that the
98 response of communities to OA is not predictable and further studies were required. Based on the
99 controversial results about OA on DMS and halocarbons production, a mesocosm experiment was
100 conducted in Wu Yuan Bay, Xiamen. The aim of this study was to investigate the influence of
101 elevated $p\text{CO}_2$ on diatoms and coccolithophores and to further understand how the productions of
102 DMS and halocarbons respond to OA.

103 **2. Experimental method**

104 *2.1 General experimental device*

105 The mesocosm experiments were carried out on a floating platform at the Facility for Ocean
106 Acidification Impacts Study of Xiamen University (FOANIC-XMU, 24.52 °N, 117.18 °E) (for full
107 technical details of the mesocosms, see Liu et al. 2017). Six cylindrical transparent thermoplastic
108 polyurethane bags with domes were deployed along the south side of the platform. The width and
109 depth of each mesocosm bag was 1.5 m and 3 m, respectively. Filtered (0.01 µm, achieved using
110 an ultrafiltration water purifier, MU801-4T, Midea, Guangdong, China) *in situ* seawater was
111 pumped into the six bags simultaneously within 24 h. A known amount of NaCl solution was
112 added to each bag to calculate the exact volume of seawater in the bags, according to a
113 comparison of the salinity before and after adding salt (Czerny et al., 2013). The initial *in situ*
114 $p\text{CO}_2$ was about 650 µatm. To set the low and high $p\text{CO}_2$ levels, we added Na_2CO_3 solution and
115 CO_2 saturated seawater to the mesocosm bags to alter total alkalinity and dissolved inorganic
116 carbon (Gattuso et al., 2010; Riebesell et al., 2013). Subsequently, during the whole experimental
117 process, air at the ambient (400 µatm) and elevated $p\text{CO}_2$ (1000 µatm) concentrations was

118 continuously bubbled into the mesocosm bags using a CO₂ Enricher (CE-100B, Wuhan Ruihua
119 Instrument & Equipment Ltd., Wuhan, China). Because the seawater in the mesocosm was filtered,
120 the algae in the coastal environment and their attached bacteria were removed and the trace gases
121 produced in the environment did not influence the mesocosm trace gas concentrations after the
122 bags were sealed.

123 2.2 Algal strains

124 *Emiliana huxleyi* (CS-369), *Phaeodactylum tricornutum* (CCMA 106), and *Thalassiosira*
125 *weissflogii* (CCMA 102) were inoculated into the mesocosm bags, with an initial
126 diatom/coccolithophorid cell ratio of 1:1. The initial concentrations of *Phaeodactylum*
127 *tricornutum*, *Thalassiosira weissflogii*, and *Emiliana huxleyi* inoculated into the mesocosm were
128 10, 10, and 20 cells mL⁻¹, respectively. *Phaeodactylum tricornutum* and *Thalassiosira*
129 *weissflogii* were obtained from the Center for Collections of Marine Bacteria and Phytoplankton
130 of the State Key Laboratory of Marine Environmental Science (Xiamen University).
131 *Phaeodactylum tricornutum* was originally isolated from the South China Sea in 2004 and
132 *Thalassiosira weissflogii* was isolated from Daya Bay in the coastal South China Sea. *Emiliana*
133 *huxleyi* was originally isolated in 1992 from the field station of the University of Bergen
134 (Raunefjorden; 60°18'N, 05°15'E). Before being introduced into the mesocosms, the three
135 phytoplankton species were cultured in autoclaved, pre-filtered seawater from Wuyuan Bay at
136 16 °C (similar to the in situ temperature of Wuyuan Bay) without any addition of nutrients.
137 Cultures were continuously aerated with filtered ambient air containing 400 µatm of CO₂ within
138 plant chambers (HP1000G-D, Wuhan Ruihua Instrument & Equipment, China) at a constant
139 bubbling rate of 300 mL min⁻¹. The culture medium was renewed every 24 h to maintain the cells

140 of each phytoplankton species in exponential growth. Meanwhile, no meaningful numbers of
141 bacteria were counted by flow cytometer in the pre-filtered seawater before the inoculations.

142 *2.3 Sampling for DMS(P) and halocarbons*

143 DMS(P) and halocarbons samples were generally obtained from six mesocosms at 9 a.m., then all
144 collected samples were transported into a dark cool box back to the laboratory onshore for
145 analysis within 1 h. For DMS analysis, 2 mL sample was gently filtered through a 25 mm GF/F
146 (glass fiber) filter and transferred to a purge and trap system linked to a Shimadzu GC-2014 gas
147 chromatograph (Tokyo, Japan) equipped with a glass column packed with 10% DEGS on
148 Chromosorb W-AW-DMCS (3 m × 3 mm) and a flame photometric detector (FPD) (Zhang et al.,
149 2014). For total DMSP analysis, 10 mL water sample was fixed using 50 µL of 50 % H₂SO₄ and
150 sealed (Kiene and Slezak, 2006). After > 1 d preservation, DMSP samples were hydrolysed for 24
151 h with a pellet of KOH (final pH > 13) to fully convert DMSP to DMS. Then, 2 mL hydrolysed
152 sample was carefully transferred to the purge and trap system mentioned above for extraction of
153 DMS. For halocarbons, 100 mL sample was purged at 40 °C with pure nitrogen at a flow rate of
154 100 mL min⁻¹ for 12 min using another purge and trap system coupled to an Agilent 6890 gas
155 chromatograph (Agilent Technologies, Palo Alto, CA, USA) equipped with an electron capture
156 detector (ECD) as well as a 60 m DB-624 capillary column (0.53 mm ID; film thickness, 3 µm)
157 (Yang et al., 2010). The analytical precision for duplicate measurements of DMS(P) and
158 halocarbons was > 10%.

159 *2.4 Measurements of chlorophyll a*

160 Chlorophyll *a* (Chl *a*) was measured in water samples (200–1,000 mL) collected every 2 d at 9
161 a.m. by filtering onto Whatman GF/F filters (25 mm). The filters were placed in 5 mL 100%

162 methanol overnight at 4 °C and centrifuged at 5000 r min⁻¹ for 10 min. The absorbance of the
163 supernatant (2.5 mL) was measured from 250 to 800 nm using a scanning spectrophotometer (DU
164 800, Beckman Coulter Inc., Brea, CA, USA). Chl *a* concentration was calculated according to the
165 equation reported by Porra (2002).

166 *2.5 Enumeration of DMSP-consuming bacteria (DCB)*

167 The number of DMSP-consuming bacteria (DCB) was estimated using the most probable number
168 (MPN) methodology. The MPN medium consisted of a mixture (1:1 v/v) of sterile artificial sea
169 water (ASW) and mineral medium (Visscher et al., 1991), 3 mL of which was dispensed in 6 mL
170 test tubes, which were closed off by an over-sized cap, allowing gas exchange. Triplicate dilution
171 series were set up. All test tubes contained 1 mmol L⁻¹ DMSP as the sole organic carbon source
172 and were kept at 30 °C in the dark. After 2 weeks, the presence/absence of bacteria in the tubes
173 was verified by DAPI staining (Porter and Feig, 1980). Three tubes containing 3 mL ASW
174 without substrate were used as controls.

175 *2.6 Statistical analysis*

176 One-way analysis of variance (ANOVA), Tukey's test, and the two-sample *t*-test were carried out
177 to demonstrate the differences between treatments. A *p*-value < 0.05 was considered significant.
178 Relationships between DMS(P), halocarbons and a range of other parameters were detected using
179 Pearson's correlation analysis via SPSS 22.0 for Windows (SPSS Inc., Chicago, IL, USA).

180 **3. Results and Discussion**

181 *3.1 Temporal changes in pH, Chl a, Phaeodactylum tricorunatum, Thalassiosira weissflogii, and* 182 *Emiliana huxleyi during the experiment*

183 During the experiment, the seawater in each mesocosm was well combined, and the temperature

184 and salinity were well controlled, with a mean of 16 °C and 29 in all mesocosms, respectively.

185 Meanwhile, we observed significant differences in pH levels between the two CO₂ treatments on

186 days 0–11, but the differences disappeared with subsequent phytoplankton growth (Fig. 1). The

187 phytoplankton growth process was divided into three phases in terms of variations in Chl *a*

188 concentrations in the mesocosm experiments as described in Liu et al. (2017): i) the logarithmic

189 growth phase (phase I, days 0–13), ii) a plateau phase (phase II, days 13–23, bloom period), and iii)

190 a secondary plateau phase (phase III, days 23–33) attained after a decline in biomass from a

191 maximum in phase II. The initial chemical parameters of the mesocosm experiment are shown in

192 Table 1. The initial mean dissolved nitrate (including NO₃⁻ and NO₂⁻), NH₄⁺, PO₄³⁻ and silicate

193 (SiO₃²⁻) concentrations were 54, 20, 2.6 and 41 μmol L⁻¹ for the low pCO₂ (LC) treatment and 52,

194 21, 2.4 and 38 μmol L⁻¹ for the high pCO₂ (HC) treatment, respectively. The nutrient

195 concentrations (NO₃⁻, NO₂⁻, NH₄⁺ and phosphate) during phase I were consumed rapidly and

196 their concentrations were below or close to the detection limit during phase II (Table 1). In

197 addition, although dissolved inorganic nitrogen (NH₄⁺, NO₃⁻, and NO₂⁻) and phosphate were

198 depleted, Chl *a* concentration in both treatments (biomass dominated by *Phaeodactylum*

199 *tricornutum*) remained constant over days 12–22, and then declined over subsequent days (Liu et

200 al., 2017). *Emiliania huxleyi* was only found in phase I and its maximal concentration reached 310

201 cells mL⁻¹ according to the results of microscopic inspection. *Thalassiosira weissflogii* was found

202 throughout the entire period in each bag, but the maximum concentration was 8,120 cells mL⁻¹,

203 which was far less than the concentration of *Phaeodactylum tricornutum* with a maximum density

204 of about 1.5 million cells mL⁻¹ (Liu et al., 2017).

205 3.2 Impact of elevated pCO₂ on DMS and DMSP production

206 At the beginning of the experiment, the mean DMS, DMSP and DCB concentrations were all low
207 in both treatments due to the low concentrations of DMS, DMSP and DCB in the original fjord
208 water and possible loss during the filtration procedure (Fig. 2). With the growth of phytoplankton,
209 DMS, DMSP and DCB showed slightly different trends during the mesocosm experiment. The
210 DMSP concentrations in the HC and LC treatments increased significantly along with the increase
211 of Chl *a* concentrations and algal cells, and stayed relatively constant over the following days. A
212 significant positive relationship was observed between DMSP and phytoplankton in the
213 experiment ($r = 0.961$, $p < 0.01$ for *Phaeodactylum tricornutum*, $r = 0.617$, $p < 0.01$ for
214 *Thalassiosira weissflogii* in the LC treatment, table 2; $r = 0.954$, $p < 0.01$ for *Phaeodactylum*
215 *tricornutum*, $r = 0.743$, $p < 0.01$ for *Thalassiosira weissflogii* in the HC treatment, table 3).
216 Compared with DMSP, DMS and DCB concentrations showed similar trends during the
217 mesocosm experiment. DMS concentrations in the LC and HC treatments were 1.03 and 0.74
218 nmol L^{-1} , respectively, while DCB concentrations in the LC and HC treatments were 0.20×10^6
219 and 0.16×10^6 cells mL^{-1} . DMS and DCB concentrations did not increase significantly during
220 phase I, but began to increase rapidly on day 15. DCB concentrations in the LC and HC treatments
221 peaked on days 21 (11.65×10^6 cells mL^{-1}) and 23 (10.70×10^6 cells mL^{-1}), while DMS
222 concentrations in the LC and HC treatments peaked on days 25 (112.1 nmol L^{-1}) and 30 (101.9
223 nmol L^{-1}). Both DMS and DCB concentrations began to decrease obviously during phase III.
224 Meanwhile, a significant positive relationship was also observed between DMS and
225 *Phaeodactylum tricornutum* ($r = 0.560$, $p < 0.05$ in the LC treatment; $r = 0.635$, $p < 0.01$ in the
226 HC treatment), while no relationship was observed between DMS and *Thalassiosira weissflogii*
227 (table 2 and table 3) during the experiment.

228 In this study, no difference in mean DMSP concentrations was observed between the two
229 treatments, indicating that elevated $p\text{CO}_2$ had no significant influence on DMSP production in
230 *Phaeodactylum tricornutum* and *Thalassiosira weissflogii* throughout this study. However, a
231 significant 29% reduction in DMS concentrations was detected in the HC treatment compared
232 with the LC treatment ($p = 0.016$), though no statistical difference for DCB concentrations was
233 found between the LC and HC treatments during phase I. This reduction in DMS concentrations
234 may be attributed to greater consumption of DMS and conversion to DMSO (Webb et al., 2015).
235 In addition, the peak DMS concentration in the HC treatment was delayed 5 days relative to that in
236 the LC treatment during phase II (Fig. 2-A). This result has been observed in previous mesocosm
237 experiments and it was attributed to small scale shifts in community composition and succession
238 that could not be identified with only a once-daily measurement regime (Vogt et al., 2008; Webb et
239 al., 2016). However, this phenomenon can be explained in another straightforward way during this
240 study. Previous studies have showed that marine bacteria play a key role in DMS production and the
241 efficiency of bacteria converting DMSP to DMS may vary from 2 to 100% depending on the
242 nutrient status of the bacteria and the quantity of dissolved organic matter (Simó et al., 2002, 2009;
243 Kiene et al., 1999, 2000). In addition, a significant positive relationship was also observed
244 between DMS and DCB ($r = 0.643$, $p < 0.01$ in the LC treatment; $r = 0.544$, $p < 0.01$ in the HC
245 treatment) during this experiment. All of these observations point to the importance of bacteria in
246 DMS and DMSP dynamics. During the present mesocosm experiment, DMSP concentrations in
247 the LC treatment decreased slightly on day 23, while the slight decrease appeared on day 29 in the
248 HC treatment (Fig. 2-B). In addition, the time that the DMSP concentration began to decrease was
249 very close to the time when the highest DMS concentration occurred in both treatments. Moreover,

250 DCB peaked on days 21 (11.65×10^6 cells mL^{-1}) and 23 (10.70×10^6 cells mL^{-1}) in the LC and
251 HC treatments, respectively, as shown in Fig. 2-C. Similar to DMS, DCB was also delayed in the
252 HC mesocosm compared to that in the LC mesocosm. Taken together, we inferred that the
253 elevated $p\text{CO}_2$ first delayed growth of DCB in the mesocosm, then the delayed DCB postponed
254 the DMSP degradation process, and eventually delayed the DMS concentration in the HC
255 treatment. In addition, considering that the algae and their attached bacteria were removed through
256 a filtering process before the experiment and the unattached bacteria were maintained in a
257 relatively constant concentration during this mesocosm experiment (Huang et al., 2018), we
258 further concluded that the elevated $p\text{CO}_2$ controlled DMS concentrations mainly by affecting DCB
259 attached to *Thalassiosira weissflogii* and *Phaeodactylum tricornutum*.

260 3.3 Impact of elevated $p\text{CO}_2$ on halocarbon compounds

261 The temporal development in CHBrCl_2 , CH_3Br , and CH_2Br_2 concentrations is shown in Fig. 3
262 (A–C) and the temporal changes of their concentrations were substantially different from those of
263 DMS, DMSP, *Phaeodactylum tricornutum* and *Thalassiosira weissflogii*. The mean
264 concentrations of CHBrCl_2 , CH_3Br and CH_2Br_2 for the entire experiment were 8.58, 7.85, and 5.13
265 pmol L^{-1} in the LC treatment and 8.81, 9.73, and 6.27 pmol L^{-1} in the HC treatment. The
266 concentrations of CHBrCl_2 , CH_3Br , and CH_2Br_2 did not increase with the Chl *a* concentration
267 compared with those of DMS and DMSP, and no major peaks were detected in the mesocosms. In
268 addition, no effect of elevated $p\text{CO}_2$ was identified for any of the three bromocarbons, which
269 compared well with previous mesocosm findings (Hopkins et al., 2010, 2013; Webb, et al., 2016).
270 No clear correlation was observed between the three bromocarbons and any of the measured algal
271 groups (table 2 and table 3), indicating that *Phaeodactylum tricornutum* and *Thalassiosira*

272 *weissflogii* did not primarily release these three bromocarbons during the mesocosm experiment.

273 Previous studies have reported that large-size cyanobacteria, such as *Aphanizomenon flos-aquae*,

274 produce bromocarbons (Karlsson et al. 2008) and significant correlations between cyanobacterium

275 abundance and several bromocarbons have been reported in the Arabian Sea (Roy et al., 2011).

276 However, the filtration procedure led to the loss of cyanobacterium in the mesocosms and finally

277 resulted in low bromocarbon concentrations during the experiment, although *Phaeodactylum*

278 *tricornuntum* and *Thalassiosira weissflogii* abundances were high.

279 The temporal dynamics of CH₃I in the HC and LC treatments are shown in Fig. 3-D. The CH₃I

280 concentrations in the LC treatment varied from 0.38 to 12.61 pmol L⁻¹, with a mean of 4.76 pmol

281 L⁻¹. The CH₃I concentrations in the HC treatment ranged between 0.44 and 8.78 pmol L⁻¹, with a

282 mean of 2.88 pmol L⁻¹. The maximum CH₃I concentrations in the HC and LC treatments were

283 both observed on day 23. The range of CH₃I concentrations during this experiment was similar to

284 that measured in the mesocosm experiment (< 1~10 pmol L⁻¹) in Kongsfjorden conducted by

285 Hopkins et al. (2013). In addition, the mean CH₃I concentration in the LC treatment was similar to

286 that measured in the East China Sea, with an average of 5.34 pmol L⁻¹ in winter and 5.74 pmol L⁻¹

287 in summer (Yuan et al., 2015). Meanwhile, a positive relationship was detected between CH₃I and

288 Chl *a*, *Phaeodactylum tricornuntum* and *Thalassiosira weissflogii* ($r = 0.588$, $p < 0.01$ in the LC

289 treatment; $r = 0.834$, $p < 0.01$ in the LC treatment for *Phaeodactylum tricornuntum*; $r = 0.680$ $p <$

290 0.01 in the LC treatment; $r = 0.690$, $p < 0.01$ in the HC treatment for *Thalassiosira weissflogii*; $r =$

291 0.717 , $p < 0.01$ in the LC treatment; $r = 0.741$, $p < 0.01$ in the HC treatment for Chl *a*). This result

292 agrees with previous mesocosm (Hopkins et al., 2013) and laboratory experiments (Hughes et al.,

293 2013; Manley and De La Cuesta, 1997) identifying diatoms as significant producers of CH₃I.

294 Moreover, similar to DMS, the maximum CH₃I concentration also occurred after the maxima of
295 *Phaeodactylum tricornutum* and *Thalassiosira weissflogii*, at about 4 d (Fig. 3-D). This was
296 similar to iodocarbon gases measured in a Norway mesocosm conducted by Hopkins et al. (2010)
297 and chloriodomethane (CH₂ClI) concentrations measured in another Norway mesocosm
298 conducted by Wingenter et al. (2007). Furthermore, the CH₃I concentrations measured in the HC
299 treatment were significantly lower than those measured in the LC treatment during the mesocosm,
300 which is in accord with the discoveries of Hopkins et al. (2010) and Webb et al. (2015) but in
301 contrast to the findings of Hopkins et al. (2013) and Webb et al. (2016). Throughout the mesocosm
302 experiment, there was a 40.2% reduction in the HC mesocosm compared to the LC mesocosm.
303 Considering that the phytoplankton species did not show significant differences in the HC and LC
304 treatments during the experiment, this reduction in the HC treatment was likely not caused by
305 phytoplankton. Apart from direct biological production via methyl transferase enzyme activity by
306 both phytoplankton and bacteria (Amachi et al., 2001), CH₃I is produced from the breakdown of
307 higher molecular weight iodine-containing organic matter (Fenical, 1982) through photochemical
308 reactions between organic matter and light (Richter and Wallace, 2004). Both bacterial methyl
309 transferase enzyme activity and a photochemical reaction may have reduced the CH₃I
310 concentrations in the HC treatment but further experiments are needed to verify this result.

311 **4. Conclusions**

312 In this study, the effects of increased levels of *p*CO₂ on marine DMS(P) and halocarbons release
313 were studied in a controlled mesocosm facility. A 28.2% reduction during the logarithmic growth
314 phase and a 5 d delay in DMS concentration was observed in the HC treatment due to the effect of
315 elevated *p*CO₂. Because the seawater in the mesocosm was filtered, the algae in the coastal

316 environment and their attached bacteria were removed and the trace gases produced in the
317 environment did not influence the mesocosm trace gas concentrations after the bags were sealed.
318 Therefore, we attribute this phenomenon to the DMSP-consuming bacteria attached to
319 *Phaeodactylum tricornutum* and *Thalassiosira weissflogii*. More attention should be paid to the
320 DMSP-consuming bacteria attached to algae under different pH values in future studies. Three
321 bromocarbons compounds were not correlated with a range of biological parameters, as they were
322 affected by the filtration procedure and elevated $p\text{CO}_2$ had no effect on any of the three
323 bromocarbons. The temporal dynamics of CH_3I , combined with strong correlations with biological
324 parameters, indicated biological control of the concentrations of this gas. In addition, the
325 production of CH_3I was sensitive to $p\text{CO}_2$, with a significant increase in CH_3I concentration at
326 higher $p\text{CO}_2$. However, without additional empirical measurements, it is unclear whether this
327 decrease was caused by bacterial methyl transferase enzyme activity or by photochemical
328 degradation at higher $p\text{CO}_2$.

329 Author contribution: Gui-Peng Yang and Kun-Shan Gao designed the experiments. Sheng-Hui
330 Zhang, Juan Yu and Qiong-Yao Ding carried out the experiments and prepared the manuscript.
331 Hong-Hai Zhang and Da-Wei Pan revised the paper.

332 **Acknowledgements**

333 This study was financially supported by the National Natural Science Foundation of China (Grant
334 Nos. 41320104008 and 41576073), the National Key Research and Development Program of
335 China (Grant No. 2016YFA0601300), the National Natural Science Foundation for Creative
336 Research Groups (Grant No. 41521064), and AoShan Talents Program of Qingdao National

337 Laboratory for Marine Science and Technology (No. 2015 ASTP). We are thankful to Minhan Dai
338 for the nutrient data and to Bangqin Huang for the bacterial data.

339 Competing interests: The authors declare that they have no conflict of interest.

340 **References**

341 Amachi, S., Kamagata, Y., Kanagawa, T., Muramatsu, Y.: Bacteria mediate methylation of iodine in marine and
342 terrestrial environments, *Appl. Environ. Microb.*, *67*, 2718–2722, 2001.

343 Archer, S. D., Kimmance, S. A., Stephens, J. A., Hopkins, F. E., Bellerby, R. G. J., Schulz, K. G., Piontek, J., Engel,
344 A.: Contrasting responses of DMS and DMSP to ocean acidification in Arctic waters, *Biogeosciences*, *10*,
345 1893–1908, 2013.

346 Avgoustidi, V., Nightingale, P. D., Joint, I., Steinke, M., Turner, S. M., Hopkins, F. E., Liss, P. S.: Decreased
347 marine dimethyl sulfide production under elevated CO₂ levels in mesocosm and in vitro studies, *Environ.*
348 *Chem.*, *9*, 399–404, 2012.

349 Bacic, M. K., Yoch, D. C.: In vivo characterization of dimethylsulfoniopropionatelyase in the fungus
350 *Fusariumlateritium*, *Appl. Environ. Microbiol.*, *64*, 106–111, 1998.

351 Boyd, P. W., Doney, S. C.: Modelling regional responses by marine pelagic ecosystems to global climate change,
352 *Geophys. Res. Lett.*, *29*, 1–4, 2002.

353 Charlson, R. J., Lovelock, J. E., Andreae, M. O., Wakeham, S. G.: Oceanic phytoplankton, atmospheric sulfur,
354 cloud albedo and climate, *Nature*, *326*, 655–661, 1987.

355 Curson, A. R., Liu, J., Bermejo Martinez, A., Green, R., Chan, Y., Carrion, O.: Dimethylsulfoniopropionate
356 biosynthesis in marine bacteria and identification of the key gene in this process, *Nat. Microbiol.*, *2*, 17009,
357 2017.

358 Czerny, J., Schulz, K. G., Ludwig, A., and Riebesell, U.: Technical Note: A simple method for air–sea gas

359 exchange measurements in mesocosms and its application in carbon budgeting, *Biogeosciences*, 10,
360 1379–1390, 2013.

361 de Souza, M. P., Yoch, D. C.: Purification and characterization of dimethylsulfoniopropionatelyase from an
362 *Alcaligenes*-like dimethyl sulfide-producing marine isolate, *Appl. Environ. Microbiol.*, 61, 21–26, 1995.

363 Doney, S. C., Fabry, V. J., Feely, R. A., Kleypas, J. A.: Ocean acidification: the other CO₂ problem, *Annu. Rev. Mar.*
364 *Sci.*, 1, 169–192, 2009.

365 Fenical, W.: Natural products chemistry in the marine environment, *Science*, 215, 923–928, 1982.

366 Gattuso, J. P., Gao, K., Lee, K., Rost, B., Schulz, K. G.: Approaches and tools to manipulate the carbonate
367 chemistry. In: Riebesell, U., et al. (Eds.), *Guide to Best Practices in Ocean Acidification Research and Data*
368 *Reporting*. Office for Official Publications of the European Communities, Luxembourg, pp. 41–52, 2010.

369 [Gattuso, J. P., Magnan, A., Bille, R., Cheung, W. W. L., Howes, E. L., Joos, F., Allemand, D., Bopp, L., Cooley, S.](#)
370 [R., Eakin, C. M., Hoegh-Guldberg, O., Kelly, R. P., Portner, H. O., Rogers, A. D., Baxter, J. M., Laffoley, D.,](#)
371 [Osborn, D., Rankovic, A., Rochette, J., Sumaila, U.R., Treyer, S., Turley, C.: Contrasting futures for ocean](#)
372 [and society from different anthropogenic CO₂ emissions scenarios, *Science*, 349 \(6243\), aac4722, 2015.](#)

373 Hopkins, F. E., Archer, S. D.: Consistent increase in dimethyl sulfide (DMS) in response to high CO₂ in five
374 shipboard bioassays from contrasting NW European waters, *Biogeosciences*, 11, 4925–4940, 2014.

375 Hopkins, F. E., Kimmance, S. A., Stephens, J. A., Bellerby, R. G. J., Brussaard, C. P. D., Czerny, J., Schulz, K. G.
376 Archer, S. D.: Response of halocarbons to ocean acidification in the Arctic, *Biogeosciences*, 10, 2331–2345,
377 2013.

378 Hopkins, F. E., Turner, S. M., Nightingale, P. D., Steinke, M., Liss, P. S.: Ocean acidification and marine biogenic
379 trace gas production, *P. Natl. Acad. Sci. USA*, 107, 760–765, 2010.

380 Huang, Y. B., Liu, X., Edward, A. L., Chen, B. Z., Li Y., Xie, Y. Y., Wu, Y. P., Gao K. S., Huang, B. Q.: Effects of

381 increasing atmospheric CO₂ on the marine phytoplankton and bacterial metabolism during a bloom: A coastal
382 mesocosm study, *Sci. Total. Environ.*, 633, 618–629, 2018.

383 Hughes, C., Johnson, M., Utting, R., Turner, S., Malin, G., Clarke, A., Liss, P. S.: Microbial control of
384 bromocarbon concentrations in coastal waters of the western Antarctic Peninsula, *Mar. Chem.*, 151, 35–46,
385 2013.

386 Jenkins, M. E., Cox, R. A., Hayman, G. D.: Kinetics of the reaction of IO radicals with HO₂ at 298 K, *Chem. Phys.*
387 *Let.*, 177, 272–278, 1991.

388 Karlsson, A., Auer, N., Schulz-Bull, D., Abrahamsson, K.: Cyanobacterial blooms in the Baltic—A source of
389 halocarbons, *Mar. Chem.*, 110, 129–139, 2008.

390 Kiene, R. P., Linn, L. J., Gonzalez, J., Moran, M. A., Bruton, J. A.: Dimethylsulfoniopropionate and methanethiol
391 are important precursors of methionine and protein-sulfur in marine bacterioplankton, *Appl. Environ.*
392 *Microbiol.*, 65, 4549–4558, 1999.

393 Kiene, R. P., Linn, L. J.: The fate of dissolved dimethylsulfoniopropionate (DMSP) in seawater: tracer studies
394 using ³⁵S-DMSP, *Geochim. Cosmochim. Acta.*, 64, 2797–2810, 2000.

395 Kiene, R. P., Slezak, D.: Low dissolved DMSP concentrations in seawater revealed by small volume gravity
396 filtration and dialysis sampling, *Limnol. Oceanogr. Methods*, 4, 80–95, 2006.

397 Kirkwood, M., Le Brun, N. E., Todd, J. D., Johnston, A. W. B.: The dddP gene of *Roseovarius nubinhibens*
398 encodes a novel lyase that cleaves dimethylsulfoniopropionate into acrylate plus dimethyl sulfide,
399 *Microbiology*, 156, 1900–1906, 2010.

400 Liss, P., Marandino, C. A., Dahl, E., Helmig, D., Hints, E. J., Hughes, C., Johnson, M., Moore, R. M., Plane, J. M.
401 C., Quack, B., Singh, H. B., Stefels, J., von Glasow, R., and Williams, J.: Short-lived trace gases in the surface
402 ocean and the atmosphere, in: *Ocean-Atmosphere Interactions of Gases and Particles*, edited by: Liss, P. and

403 Johnson, M., 55–112, 2014.

404 Liu, N., Tong, S., Yi, X., Li, Y., Li, Z., Miao, H., Wang, T., Li, F., Yan, D., Huang, R., Wu, Y., Hutchins, D. A.,
405 Beardall, J., Dai, M., Gao, K.: Carbon assimilation and losses during an ocean acidification mesocosm
406 experiment, with special reference to algal blooms, *Mar. Environ. Res.*, 129, 229–235, 2017.

407 Manley, S. L., De La Cuesta, J. L.: Methyl iodide production from marine phytoplankton cultures, *Limnol.*
408 *Oceanogr.*, 42, 142–147, 1997.

409 Orr, J. C., Fabry, V. J., Aumont, O., Bopp, L., Doney, S. C., Feely, R. A., Gnanadesikan, A., Gruber, N., Ishida,
410 A., Joos, F., Key, R. M., Lindsay, K., Maier-Reimer, E., Matear, R., Monfray, P., Mouchet, A., Najjar, R.,
411 G., Plattner, G. K., Rodgers, K. B., Sabine, C. L., Sarmiento, J. L., Schlitzer, R., Slater, R. D., Totterdell, I.
412 J., Weirig, M. F., Yamanaka, Y., Yool, A.: Anthropogenic ocean acidification over the twenty first century and
413 its impact on calcifying organisms, *Nature*, 437, 681–686, 2005.

414 [Porra, R. J.: The chequered history of the development and use of simultaneous equations for the accurate
415 determination of chlorophylls a and b, *Photosynth. Res.*, 73, 149–156, 2002.](#)

416 [Porter, K. G., Feig, Y. S.: DAPI for identifying and counting aquatic microflora, *Limnol. Oceanogr.*, 25, 946–948,
417 1980.](#)

418 Quinn, P. K., Bates, T. S.: The case against climate regulation via oceanic phytoplankton sulphur emissions, *Nature*,
419 480, 51–56, 2011.

420 [Raina, J. B., Tapiolas, D., Motti, C. A., Foret, S., Seemann, T., Tebben, J.: Isolation of an antimicrobial compound
421 produced by bacteria associated with reef-building corals, *PeerJ*, 4, e2275, 2016](#)

422 Richter, U., Wallace, D. W. R.: Production of methyl iodide in the tropical Atlantic Ocean, *Geophys. Res. Lett.*, 31,
423 L23S03, doi:10.1029/2004GL020779, 2004.

424 Riebesell, U., Czerny, J., von Brckel, K., Boxhammer, T., B üdenbender, J., Deckelnick, M., Fischer, M.,

425 Hoffmann, Krug, S. A., Lentz, U., Ludwig, A., Muche, R., Schulz, K. G.: Technical Note: a mobile sea-going
426 mesocosm system-new opportunities for ocean change research, *Biogeosciences*, 10, 1835–1847, 2013.

427 Roy, R., Pratihary, A., Narvenkar, G., Mochemadkar, S., Gauns, M., Naqvi, S. W. A.: The relationship between
428 volatile halocarbons and phytoplankton pigments during a *Trichodesmium* bloom in the coastal eastern
429 Arabian Sea, *Estuar. Coast. Shelf Sci.*, 95, 110–118, 2011.

430 Simó, R., Archer, S. D., Pedros-Alio, C., Gilpin, L., StelfoxWiddicombe, C. E.: Coupled dynamics of
431 dimethylsulfoniopropionate and dimethylsulfide cycling and the microbial food web in surface waters of the
432 North Atlantic, *Limnol. Oceanogr.*, 47, 53–61, 2002.

433 Simó, R., Vila-Costa, M., Alonso-Sáez, L., Cardelús, C., Guadayol, Ó., Vázquez-Dominguez, E., Gasol, J. M.:
434 Annual DMSP contribution to S and C fluxes through phytoplankton and bacterioplankton in a NW
435 Mediterranean coastal site, *Aquat. Microb. Ecol.*, 57, 43–55, 2009.

436 Stefels, J., Dijkhuizen, L.: Characteristics of DMSP-lyase in *Phaeocystis* sp. (Prymnesiophyceae), *Mar. Ecol. Prog.*
437 *Ser.*, 131, 307–313, 1996.

438 Stefels, J., Steink, M., Turner, S., Malin, G., Belviso, S.: Environmental constraints on the production of the
439 climatically active gas dimethylsulphide (DMS) and implications for ecosystem modeling, *Biogeochemistry*,
440 83, 245–275, 2007.

441 Steinke, M., Kirst, G. O.: Enzymatic cleavage of dimethylsulfoniopropionate (DMSP) in cell-free extracts of the
442 marine macroalga *Enteromorpha clathrata* (Roth) Grev (Ulvales, Chlorophyta), *J. Exp. Mar. Biol. Ecol.*, 201,
443 73–85, 1996.

444 Todd, J. D., Rogers, R., Li, Y. G., Wexler, M., Bond, P. L., Sun, L., Cruson, A. R. J., Malin, G., Steinke, M.,
445 Johnston, A. W. B.: Structural and regulatory genes required to make the gas dimethyl sulfide in bacteria,
446 Science, 315, 666–669, 2007.

447 Visscher, P. T., Quist, P., van Gemerden, H.: Methylated sulfur compounds in microbial mats: in situ
448 concentrations and metabolism by a colorless sulfur bacterium, *Appl. Environ. Microbiol.*, 57, 1758–1763,
449 1991.

450 Vogt, M., Steinke, M., Turner, S. M., Paulino, A., Meyerhöfer, M., Riebesell, U., LeQuéré C., Liss, P. S.:
451 Dynamics of dimethylsulphoniopropionate and dimethylsulphide under different CO₂ concentrations during
452 a mesocosm experiment, *Biogeosciences*, 5, 407–419, 2008.

453 Webb, A. L., Leedham-Elvidge, E., Hughes, C., Hopkins, F. E., Malin, G., Bach, L. T., Schulz, K., Crawford, K.,
454 Brussaard, C. P. D., Stühr, A., Riebesell, U., Liss, P. S.: Effect of ocean acidification and elevated *f* CO₂ on
455 trace gas production by a Baltic Sea summer phytoplankton community, *Biogeosciences*, 13, 4595–4613,
456 2016.

457 Webb, A. L., Malin, G., Hopkins, F. E., Ho, K. L., Riebesell, U., Schulz, K., Larsen, A., Liss, P.: Ocean
458 acidification has different effects on the production of dimethylsulphide and dimethylsulphoniopropionate
459 measured in cultures of *Emiliana huxleyi* RCC1229 and mesocosm study: a comparison of laboratory
460 monocultures and community interactions, *Environ. Chem.*, 13, EN14268, doi:10.1071/EN14268, 2015.

461 Wingenter, O. W., Haase, K. B., Zeigler, M., Blake, D. R., Rowland, F. S., Sive, B. C., Paulino, A., Thyrhaug, R.,
462 Larsen, A., Schulz K., Meyerhofer, M., Riebesell, U.: Unexpected consequences of increasing CO₂ and ocean
463 acidity on marine production of DMS and CH₂Cl₂: Potential climate impacts, *Geophys. Res. Lett.*, 34,
464 L05710, 2007.

465 Yang, G. P., Lu, X. L., Song, G. S., Wang, X. M.: Purge-and-trap gas chromatography method for analysis of
466 methyl chloride and methyl bromide in seawater, *Chin. J. Anal. Chem.*, 38 (5), 719–722. 2010.

467 Yost, D. M., Mitchelmore, C. L.: Dimethylsulfoniopropionate (DMSP) lyase activity in different strains of the
468 symbiotic alga *Symbiodinium microadriaticum*, *Mar. Ecol. Prog. Ser.*, 386, 61–70, 2009.

469 Yuan, D., Yang, G. P., He, Z.: Spatio-temporal distributions of chlorofluorocarbons and methyl iodide in the
470 Changjiang (Yangtze River) estuary and its adjacent marine area, *Mar. Pollut. Bull.*, 103 (1-2), 247–259,
471 2016.

472 Zhang, S. H., Yang, G. P., Zhang, H. H., Yang, J.: Spatial variation of biogenic sulfur in the south Yellow Sea and
473 the East China Sea during summer and its contribution to atmospheric sulfate aerosol, *Sci. Total Environ.*,
474 488–489, 157–167, 2014.

475

476

477

Figure captions

478 Fig. 1 Temporal changes of pH in the HC (1,000 μatm , solid squares) and LC (400 μatm , white
479 squares) mesocosms (3,000 L). Data are mean \pm standard deviation, $n = 3$ (triplicate independent
480 mesocosm bags) (Origin 8.0).

481 Fig. 2 Temporal changes in DMS, DMSP and DCB concentrations in the HC (1,000 μatm , black
482 squares) and LC (400 μatm , white squares) mesocosms (3,000 L). Data are mean \pm standard
483 deviation, $n = 3$ (triplicate independent mesocosm bags).

484 Fig. 3 Temporal changes in CHBrCl_2 , CH_3Br , CH_2Br_2 and CH_3I concentrations in the HC (1,000
485 μatm , black squares) and LC (400 μatm , white squares) mesocosms (3,000 L). Data are mean \pm
486 standard deviation, $n = 3$ (triplicate independent mesocosm bags).

487

488

489

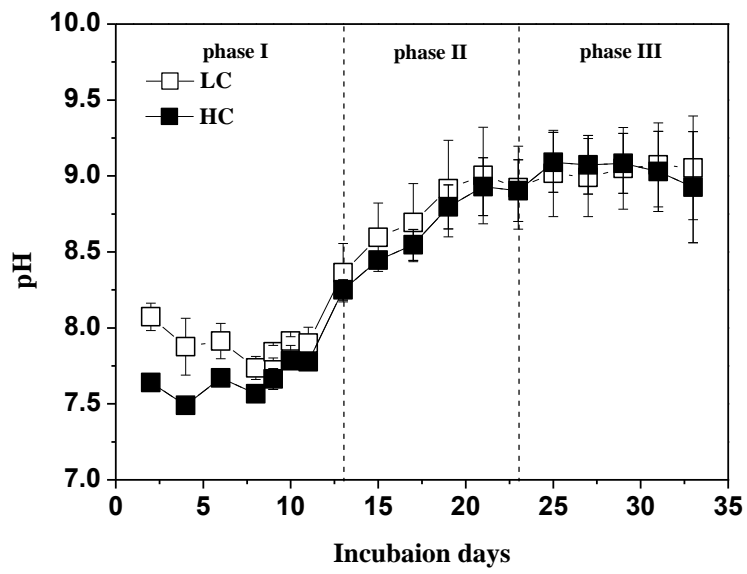
490

491

492

493

494



495

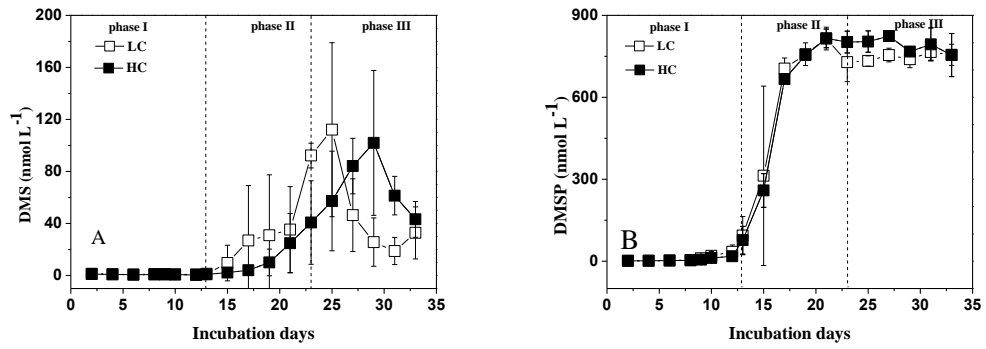
496 **Fig. 1.** Temporal changes of pH in the HC (1,000 μatm, solid squares) and LC (400 μatm, white squares)

497 mesocosms (3,000 L). Data are mean ± standard deviation, n = 3 (triplicate independent mesocosm bags) (Origin

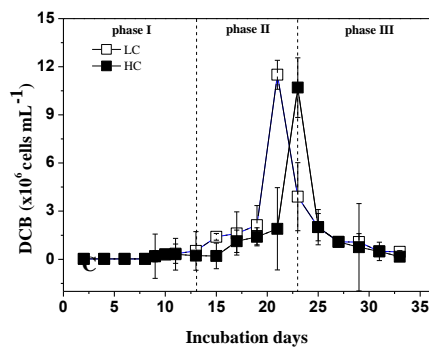
498 8.0).

499

500



501



502

503 **Fig. 2** Temporal changes in DMS (A), DMSP (B), DCB (C) concentrations in the HC (1,000 μatm , black squares)
504 and LC (400 μatm , white squares) mesocosms (3,000 L). Data are mean \pm standard deviation, n = 3 (triplicate
505 independent mesocosm bags) (Origin 8.0).

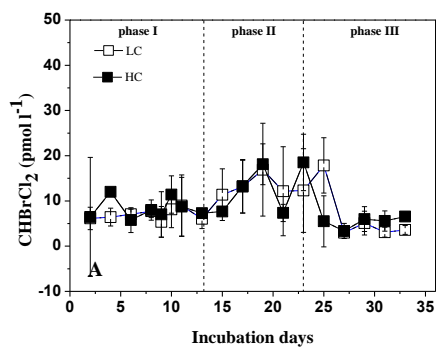
506

507

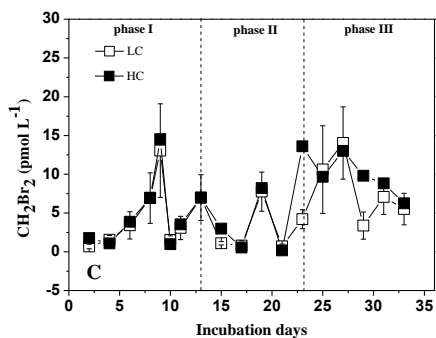
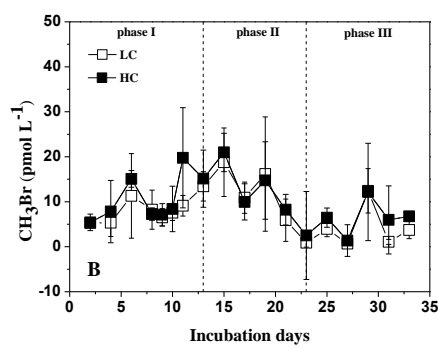
508

509

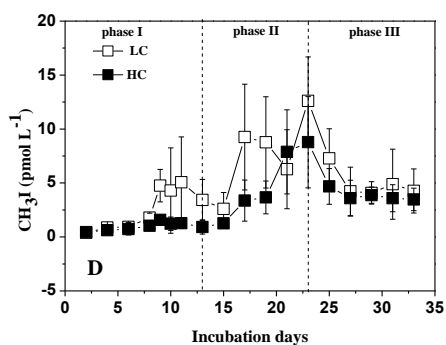
510



511



512



513 **Fig. 3** Temporal changes in CHBrCl_2 (A), CH_3Br (B), CH_2Br_2 (C) and CH_3I (D) concentrations in the HC (1,000
 514 μatm , black squares) and LC (400 μatm , white squares) mesocosms (3,000 L). Data are mean \pm standard deviation,
 515 $n = 3$ (triplicate independent mesocosm bags) (Origin 8.0).

516

517 **Table 1.** The conditions of DIC, pH_T , pCO_2 and nutrient concentrations in the mesocosm experiments. “-” means
 518 that the values were below the detection limit.

		pH_T	DIC ($\mu\text{mol kg}^{-1}$)	pCO_2 (μatm)	$NO_3^-+NO_2^-$ ($\mu\text{mol L}^{-1}$)	NH_4^+ ($\mu\text{mol L}^{-1}$)	PO_4^{3-} ($\mu\text{mol L}^{-1}$)	SiO_3^{2-} ($\mu\text{mol L}^{-1}$)
day 0	LC	8.0 \pm 0.1	2181 \pm 29	1170~1284	52~56	19~23	2.6 \pm 0.2	38~40
	HC	7.5 \pm 0.1	2333 \pm 34	340~413	51~55	19~23	2.5 \pm 0.2	38~39
Phase I	LC	7.9~8.4	1825~2178	373~888	15~52	1.6~20	0.5~2.6	31~38
	HC	7.4~8.2	2029~2338	1295~1396	47~54	0.2~21	0.7~2.5	34~39
Phase II	LC	8.4~8.5	1706~1745	46~749	-- 15.9	-	0.1~0.5	10~24
	HC	8.4~8.6	1740~1891	59~1164	1.1~25	-	--0.1	29~30
Phase III	LC	8.5~8.8	1673~1706	30~43	-	-	-	10~16
	HC	8.6~8.7	1616~1740	34~110	-	-	--0.3	24~25

519

520 **Table 2.** Relationships between DMS, DMSP, Chl *a*, CHBrCl₂, CH₃Br, CH₂Br₂, CH₃I, DCB, *Thalassiosira weissflogii* (*T. weissflogii*) and *Phaeodactylum tricorutum* (*P. tricorutum*)
 521 concentrations in the LC treatments.

	DMS (nmol L ⁻¹)	DMSP (nmol L ⁻¹)	Chl <i>a</i> (µg L ⁻¹)	CHBrCl ₂ (pmol L ⁻¹)	CH ₃ Br (pmol L ⁻¹)	CH ₂ Br ₂ (pmol L ⁻¹)	CH ₃ I (pmol L ⁻¹)	DCB (×10 ⁶ cells mL ⁻¹)	<i>T. weissflogii</i> (×10 ³ cells mL ⁻¹)	<i>P. tricorutum</i> (cells mL ⁻¹)
DMS	1									
DMSP	0.701**	1								
Chl <i>a</i>	0.597**	0.792**	1							
CHBrCl ₂	0.526	0.280	0.559	1						
CH ₃ Br	-0.413	-0.230	0.196	0.313	1					
CH ₂ Br ₂	0.310	0.180	0.001	-0.136	-0.308	1				
CH ₃ I	0.694**	0.654**	0.717**	0.596*	-0.151	0.129	1			
DCB	0.643**	0.520*	0.522*	0.394	-0.268	-0.038	0.762**	1		
<i>T. weissflogii</i>	0.410	0.617**	0.899**	0.301	0.322	0.028	0.680**	0.399	1	
<i>P. tricorutum</i>	0.560*	0.961**	0.821**	0.528	-0.032	0.162	0.588**	0.334	0.685**	1

522

523

524

525

526

527

528 **Table 3.** Relationships between DMS, DMSP, Chl *a*, CHBrCl₂, CH₃Br, CH₂Br₂, CH₃I, DCB, *Thalassiosira weissflogii* (*T. weissflogii*) and *Phaeodactylum tricornutum* (*P. tricornutum*)

529 concentrations in the HC treatments.

	DMS (nmol L ⁻¹)	DMSP (nmol L ⁻¹)	Chl <i>a</i> (µg L ⁻¹)	CHBrCl ₂ (pmol L ⁻¹)	CH ₃ Br (pmol L ⁻¹)	CH ₂ Br ₂ (pmol L ⁻¹)	CH ₃ I (pmol L ⁻¹)	DCB (×10 ⁶ cells mL ⁻¹)	<i>T. weissflogii</i> (×10 ³ cells mL ⁻¹)	<i>P. tricornutum</i> (cells mL ⁻¹)
DMS	1									
DMSP	0.752**	1								
Chl <i>a</i>	0.318*	0.738**	1							
CHBrCl ₂	0.324	0.094	0.326	1						
CH ₃ Br	-0.410	-0.349	0.065	0.076	1					
CH ₂ Br ₂	0.540*	0.352	0.142	0.233	-0.377	1				
CH ₃ I	0.694**	0.816**	0.741**	0.690*	-0.407	0.316	1			
DCB	0.544*	0.522	0.549*	0.532	-0.311	0.368	0.851*	1		
<i>T. weissflogii</i>	0.355	0.743**	0.930**	0.304	0.076	0.233	0.690**	0.567	1	
<i>P. tricornutum</i>	0.635**	0.954**	0.803**	0.143	-0.257	0.267	0.834**	0.559	0.820**	1

530

531